

Modal description—A better way of characterizing human vibration behavior

Sebastian Rützel^{a,*}, Barbara Hinz^b, Horst Peter Wölfel^a

^a*Department of Structural Dynamics, Darmstadt University of Technology, Petersenstrasse 30, D-64287 Darmstadt, Germany*

^b*Federal Institute for Occupational Safety and Health, Nöldnerstr. 40–42, D-10317 Berlin, Germany*

Received 2 May 2006; received in revised form 10 May 2006; accepted 8 June 2006

Available online 31 July 2006

Abstract

Biodynamic responses to whole body vibrations are usually characterized in terms of transfer functions, such as impedance or apparent mass. Data measurements from subjects are averaged and analyzed with respect to certain attributes (anthropometrics, posture, excitation intensity, etc.). Averaging involves the risk of identifying unnatural vibration characteristics.

The use of a modal description as an alternative method is presented and its contribution to biodynamic modelling is discussed. Modal description is not limited to just one biodynamic function: The method holds for all transfer functions. This is shown in terms of the apparent mass and the seat-to-head transfer function.

The advantages of modal description are illustrated using apparent mass data of six male individuals of the same mass percentile. From experimental data, modal parameters such as natural frequencies, damping ratios and modal masses are identified which can easily be used to set up a mathematical model. Following the phenomenological approach, this model will provide the global vibration behavior relating to the input data.

The modal description could be used for the development of hardware vibration dummies. With respect to software models such as finite element models, the validation process for these models can be supported by the modal approach. Modal parameters of computational models and of the experimental data can establish a basis for comparison.

© 2006 Elsevier Ltd. All rights reserved.

1. Introduction

As a result of increasing mobility, humans face a multiplicity of vibrations in vehicles or at the workplace. One can divide these oscillations into two categories:

- they may reduce the comfort of the occupants, or
- they may lead to serious physical injuries.

*Corresponding author. Tel.: +49 6151 164061.

E-mail address: ruetzel@fmd.tu-darmstadt.de (S. Rützel).

Vibrational comfort and damage due to oscillations have become an important issue for two different reasons:

- since diseases of the lumbar spine/cervical spine resulting from exposure to vibration at the workplace were acknowledged as occupational disease within the last decade, an employee may sue the employer for damages [1,2].
- with rising expectations of customers, and unification of car concepts, comfort is one key area in which car manufacturers can achieve differentiation with respect to competitors. Numerous approaches have been proposed to objectify comfort.

The two latter aspects have led to a growing demand for research and an interest in a systematic analysis of the human body. On the one hand, invasive experiments on humans are limited by ethic concerns. On the other hand, results from questionnaires vary with the subjectivity of test persons (TP) and show a lack of reproducibility.

Thus, there are good reasons to develop biodynamic models of man. Simulation results of these models will help to understand the behavior of the human body and to estimate the consequences of exposure to vibration.

In order to draw a conclusion it is essential that the models provide reliable results. Therefore, all biodynamic models—phenomenological and anatomical—need to be validated carefully. This study presents a method which can improve the quality of models and make them comparable. An identification technique based on modal decomposition is proposed, which extracts the significant dynamic properties of the human body from measured response functions.

Several phenomenological models have been proposed, based on experimental biodynamic data. Fig. 1 shows a selection of different models designed to represent a sitting human subject exposed to vertical vibration.

A variety of structures with one or multiple degrees of freedom were presented in Refs. [3–8] and defined in the standard ISO 5982 [9]. Models for horizontal vibration can be derived in an analog manner [10].

Wei and Griffin [8] investigated a two dof parallel model which has the same structure as the model of Suggs et al. [4]. The models 1b and 2b proposed by Wei and Griffin [8] fulfill the requirements of a modal model in terms of the structure which will be described in detail in Section 2.2. In Ref. [8], modal parameters such as modal mass, modal stiffness and modal damping coefficients are identified and averaged within a group (i.e., men, women and children), but the idea of the modal approach is not mentioned. However, the authors conclude that both modal models (1b, 2b) yielded better results for representing the apparent masses of the input data than the models without a rigid support (1a, 2a).

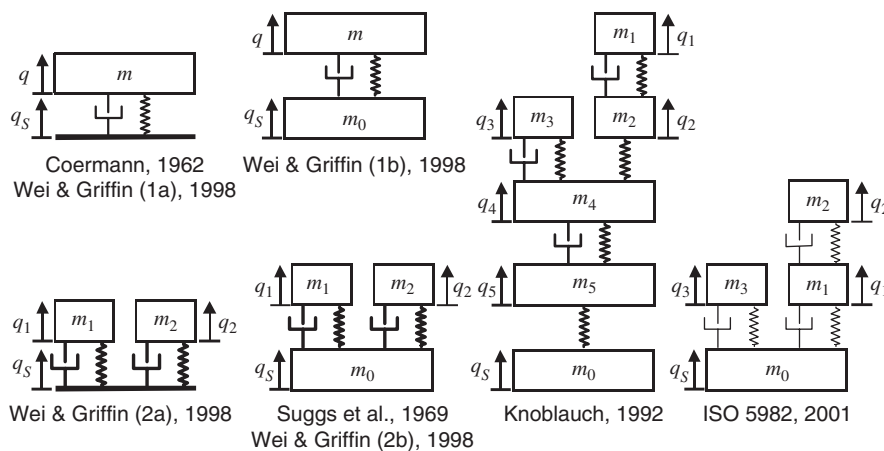


Fig. 1. Selection of phenomenological models.

2. Method

2.1. Characteristics of whole-body vibrations

The most common function with respect to whole body vibrations is the apparent mass, defined as

$$M(\Omega) = \frac{F(\Omega)}{\ddot{Q}(\Omega)} \quad \text{with } \Omega = 2\pi f. \quad (1)$$

This apparent mass is the ratio, in the frequency domain, of the complex force to the complex vibration acceleration, measured at the same point and in the same direction as the force [9]. In this paper, we concentrate on the forces and accelerations of a seated human under vertical vibration at the man-seat interface in the z -direction, illustrated in Fig. 2.

Some authors have reported biodynamic response functions in terms of the driving-point mechanical impedance, which has some advantages for the visual representation of higher frequencies. The relationship between the impedance and apparent mass is determined by the fixed factor $j\Omega$:

$$I(\Omega) = j\Omega M(\Omega). \quad (2)$$

If the vibration behavior of the human body itself is to be analyzed, the biodynamic response function has to be measured on a rigid seat. Fig. 2 shows the experimental setup.

The vibration response depends on a variety of parameters; the following quantities have the most influence:

- anthropometrics (body mass, mass distribution, body height, etc.),
- posture,
- intensity of excitation,
- direction of excitation,
- gender.

Descriptions of vibration behavior, commonly classify TP and group them in percentiles, according to weight or height.

Usually, a mean function is calculated, although averaging involves the risk of equalizing certain characteristics, i.e. peaks are lost or the frequency range of peaks is shifted.

These effects can be observed in the standard ISO 5982 [9], which defines a mean apparent mass and driving-point mechanical impedance, respectively. The modulus of the impedance in Fig. 3 is very flat in the frequency range between 5 and 14 Hz. The upper and lower limits indicate that the original data contained more variability in impedance curves, because the mean curve was computed from measurements of 101 subjects, with a body mass ranging from 49 to 93 kg. The excitation intensities varied between 0.5 and 3.0 m s^{-2} rms.

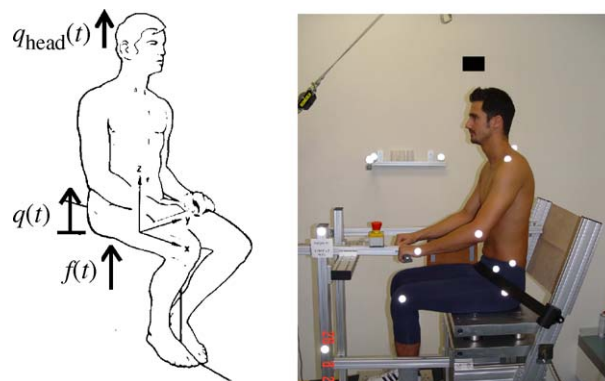


Fig. 2. Measurements on the test person, experimental setup.

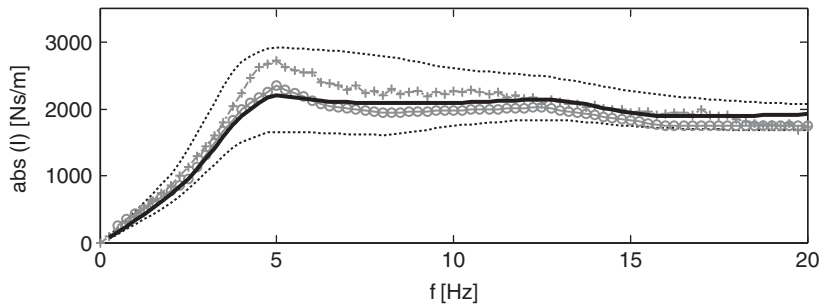


Fig. 3. Driving-point impedance of ISO 5982 [9]. — mean, upper and lower limit, -+- Fairley and Griffin, 75 kg, —o— Boileau et al., 70 kg.

2.2. Modal description of biodynamic response functions

The use of modal identification techniques can help to overcome problems which arise from data averaging.

The human body can be represented as model which contains a base mass m_0^m and n sets of single-degree-of-freedom (sdof) structures consisting of a mass m_r^m , a spring k_r^m and a damper c_r^m , where the superscript m refers to the modal model. This approach implies a very simple requirement: The given system must be able to be mapped to a linear model. Linearity of the system itself is not a requisite. To cover nonlinear effects of the human body, it is necessary to develop vibration intensity-dependent models and to identify different sets of modal parameters.

The unique feature of a modal model is its structure. Thus, no effort is needed to find the “best model structure” of a system (arrangement of several degrees of freedom in series and/or in parallel). By definition, the modal approach includes all dynamic properties in a certain frequency range. It is essential to decide how many and which modes are taken into account. The number of modes equals the sdof sets.

The apparent mass of the model shown in Fig. 4 can be calculated as

$$M(\Omega) = m_0^m + \sum_{r=1}^n m_r^m V_r(\Omega), \tag{3}$$

where $V_r(\Omega)$ denotes the frequency response function of each base-excited sdof system:

$$V_r(\Omega) = \frac{1 + j2D_r(\Omega/\omega_r)}{1 - (\Omega/\omega_r)^2 + j2D_r(\Omega/\omega_r)}. \tag{4}$$

Eq. (4) contains the parameters which represent all the dynamic components of each sdof structure:

- natural frequencies $f_r = \omega_r/2\pi$ (Hz),
- damping ratios $D_r = \frac{1}{2}c_r^m/\sqrt{m_r^m k_r^m}$ (dimensionless).

The natural frequencies and the damping ratios in Eq. (4) can be replaced by terms of the modal stiffness and the modal damping coefficients.

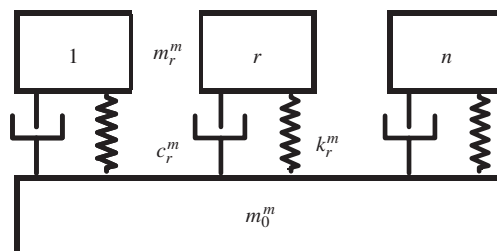


Fig. 4. Biodynamic model of the seated human body—modal approach.

Each frequency response function is multiplied by the corresponding modal mass m_r^m (kg). Finally, the base mass m_0^m (kg) is added to the apparent mass.

From the apparent mass curves, limits both at the lower and at the upper frequency range can easily be identified:

$$M(\Omega \rightarrow 0) = m_0^m + \sum m_r^m, \quad (5)$$

$$M(\Omega \rightarrow \infty) = m_0^m. \quad (6)$$

The disadvantage of the common averaging method is evident in Fig. 5, where the apparent mass curves of two sdof models with rigid support are plotted. The parameters are chosen so that they reveal the differences between averaging and modal averaging. Both models have the same masses ($m_0 = 10$ kg and $m_1 = 25$ kg), but the natural frequency and the damping ratio vary slightly between model A ($f_{1,A} = 5$ Hz, $D_{1,A} = 0.1$) and model B ($f_{1,B} = 6.5$ Hz, $D_{1,B} = 0.12$). The mean apparent mass curve of models A and B exhibits two clear peaks. If one was to identify the model parameters of the averaged function, one would use a structure with two degrees of freedom. Thus, an unnatural vibration characteristic would be determined since the input data only consists of sdof systems. Modal averaging can overcome the problem: The averaged function preserves the characteristic of an sdof structure.

The number of natural frequencies contributing to the target function $M(\Omega)$ can be chosen as necessary. Theoretically, the apparent mass function in Eq. (3) contains a sum of infinite sdof structures. The higher the number of degrees of freedom, the better the modal model approximates the original data. The risk associated with too many degrees of freedom is that unnatural vibration modes are identified which probably do not originate in the human body itself. This is not caused by the mode decoupling method itself, but by the identification algorithm.

This method is useful for the identification of the main biodynamic characteristics, i.e. the global natural frequencies. Therefore, it is appropriate to select a certain number n with regard to the measured transfer function. The course of the curves mainly depends on the direction of excitation/direction of measurement. For the vertical direction, it was observed that three sdof structures are usually sufficient to reproduce a given apparent mass curve in a frequency range up to 30 Hz. Generally speaking, the number of relevant resonances

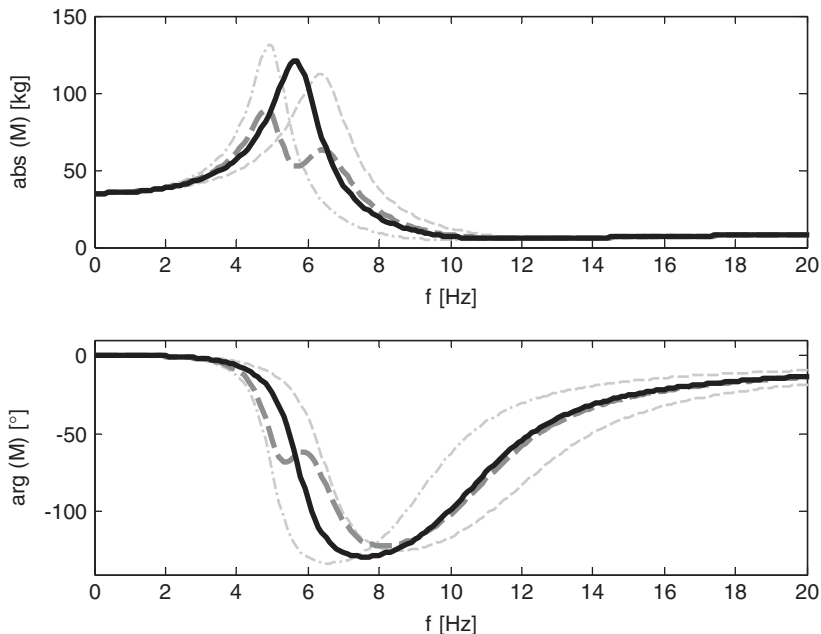


Fig. 5. ----- apparent mass of sdof model A , ----- apparent mass of sdof model B , - - - mean apparent mass of both models, ——— modally averaged apparent mass of both models.

can be better detected from the phase response than from the modulus (cf. Fig. 10). The third resonance is not very clear in the modulus because of the high damping in the frequency range above 20 Hz, but nevertheless the phase shift is evident in Fig. 10. Under horizontal excitation, the response functions include one or two main resonances, depending on the vibration intensity (cf. Hinz et al. [11]).

The identification algorithm is based on the minimization of error functions expressed in terms of apparent mass errors. The objective function is defined as

$$\sum_{\Omega} |M_{\text{identified}}(\Omega) - M_{\text{data}}(\Omega)|^2 = E. \quad (7)$$

A common least-square optimization technique is utilized to minimize the error E using MATLAB [12]. The minimization problem, expressed in Eq. (7), is solved by applying constraints to the target vector $[f_r, D_r, m_r^m, m_0^m]$. The constraints are simply inequalities, i.e. all parameters must be greater than zero. The target vector contains all modal parameters which are needed to calculate the apparent mass according to the model in Fig. 4. The vector has the length of $3n + 1$ where n denotes the total number of degrees of freedom. It is evident that the lower bound constraints the parameters to be positive numbers.

To obtain the global minimum of the objective function, we implemented an iterative identification process which varies the starting values of the modal parameters' vector and compares the identified results with the previous ones.

2.3. The relation between various transfer functions

Besides the driving-point mechanical impedance and the apparent mass, another biodynamic response function, the seat-to-head transmissibility function, is commonly used. It is defined as the complex ratio of the motion of the head to the motion at the man-seat interface as shown in Fig. 2:

$$H(\Omega) = \frac{Q_{\text{head}}(\Omega)}{Q(\Omega)} = \frac{\ddot{Q}_{\text{head}}(\Omega)}{\ddot{Q}(\Omega)}. \quad (8)$$

Other transfer functions, such as the response of the acromion or of a vertebra to an excitation of the buttocks, are rarely found in the literature.

Some mathematical models cover both the seat-to-head transfer function and the function describing the interaction of the human body with respect to the seat. Various authors created structures where one mass (degree of freedom) can be associated with the head. For example, ISO 5982 denotes m_2 as the representation of the head. Wu et al. [13] studied the relationships between biodynamic response functions and considered several models [3–5] which were derived to represent the “to-the-body” response, such as impedance or apparent mass. Expressions to describe the relation between apparent mass and seat-to-head transfer function were proposed.

The following example aims to demonstrate that the modal description holds for the seat-to-head transfer function as well. A model consisting of three degrees of freedom connecting masses, springs, and dampers in series and a model with three parallel sdof structures (according to the German standard 45 676 [14]) are shown in Fig. 6.

The stiffness and mass parameters of the in series model, which are given in Table 1, are derived from a synthetic apparent mass curve. Even if the human body does not show a damping behavior which can be described as proportional damping, this example employs a factor proportional to the stiffness matrix, for clarity ($\mathbf{C} = 0.005 \cdot \mathbf{K}$).

If the modal description method were applied to a non-classically damped system (i.e. a dynamic system without proportional damping), a decoupling approximation is required. Several methods were developed to find an estimation of a diagonalized damping matrix [15–17].

The apparent mass function of the 3 dof in series model (Fig. 6 left) can be calculated by solving the lower line of Eq. (9) for \mathbf{f}^0 . Double differentiation with respect to $j\Omega$ yields the simulated response at the base mass depicted in Fig. 7.

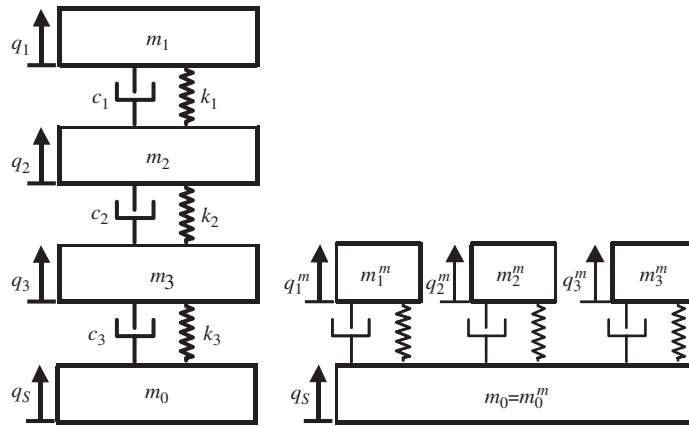


Fig. 6. 3 dof in series model, model with 3 modal dof.

Table 1

Parameters of 3 dof in series model; parameters of 3 dof modal model; natural frequencies and damping ratios of both models (series and modal)

Series model		Modal model		Both models	
Parameter	Value	Parameter	Value	Parameter	Value
m_0 (kg)	10.37	m_0^m (kg)	10.37	f_1 (Hz)	5.9
m_1 (kg)	12.56	m_1^m (kg)	23.45	f_2 (Hz)	13.1
m_2 (kg)	16.6	m_2^m (kg)	12.12	f_3 (Hz)	33.5
m_3 (kg)	9.56	m_3^m (kg)	3.16	D_1 (%)	9.3
k_1 (N/m)	24105	k_1^m (N/m)	32678	D_2 (%)	20.6
k_2 (N/m)	136080	k_2^m (N/m)	82375	D_3 (%)	52.6
k_3 (N/m)	254700	k_3^m (N/m)	139650		
c_1 (N s/m)	120.53	c_1^m (N s/m)	163.39		
c_2 (N s/m)	680.4	c_2^m (N s/m)	411.87		
c_3 (N s/m)	1273.5	c_3^m (N s/m)	698.24		

The equation of motion for a base excited structure (in the present case $\mathbf{f} = 0$) can be expressed as

$$\begin{bmatrix} \mathbf{M} & \mathbf{M}^0 \\ \mathbf{M}^{0T} & \mathbf{M}^{00} \end{bmatrix} \begin{bmatrix} \ddot{\mathbf{q}} \\ \ddot{\mathbf{q}}^0 \end{bmatrix} + \begin{bmatrix} \mathbf{C} & \mathbf{C}^0 \\ \mathbf{C}^{0T} & \mathbf{C}^{00} \end{bmatrix} \begin{bmatrix} \dot{\mathbf{q}} \\ \dot{\mathbf{q}}^0 \end{bmatrix} + \begin{bmatrix} \mathbf{K} & \mathbf{K}^0 \\ \mathbf{K}^{0T} & \mathbf{K}^{00} \end{bmatrix} \begin{bmatrix} \mathbf{q} \\ \mathbf{q}^0 \end{bmatrix} = \begin{bmatrix} \mathbf{f} \\ \mathbf{f}^0 \end{bmatrix}. \tag{9}$$

All dynamic properties for the eigenvalue analysis are included in the system matrices \mathbf{M} , \mathbf{C} and \mathbf{K} . The eigenvalue problem reads as follows:

$$(\lambda_r^2 \mathbf{M} + \lambda_r \mathbf{C} + \mathbf{K}) \boldsymbol{\varphi}_r = 0, \tag{10}$$

where λ_r denotes the r th eigenvalue and $\boldsymbol{\varphi}_r$ the r th eigenvector. To solve the eigenvalue problem, the equation of motion (9) can be transformed into a set of first-order differential equations:

$$\dot{\mathbf{z}} = \mathbf{A} \mathbf{z} \tag{11}$$

with the system matrix \mathbf{A}

$$\mathbf{A} = \begin{bmatrix} \mathbf{0} & \mathbf{I} \\ -\mathbf{M}^{-1} \mathbf{K} & -\mathbf{M}^{-1} \mathbf{C} \end{bmatrix}. \tag{12}$$

Then, the solution of the eigenvalue problem yields the eigenvalues which are usually complex numbers, as well as the right \mathbf{r} and left \mathbf{l} eigenvectors. In the following, the right eigenvectors are used and denoted as $\boldsymbol{\varphi}$:

$$(\mathbf{A} - \lambda \mathbf{I}) \mathbf{r} = \mathbf{0}, \quad (\mathbf{A}^T - \lambda \mathbf{I}) \mathbf{l} = \mathbf{0}. \tag{13}$$

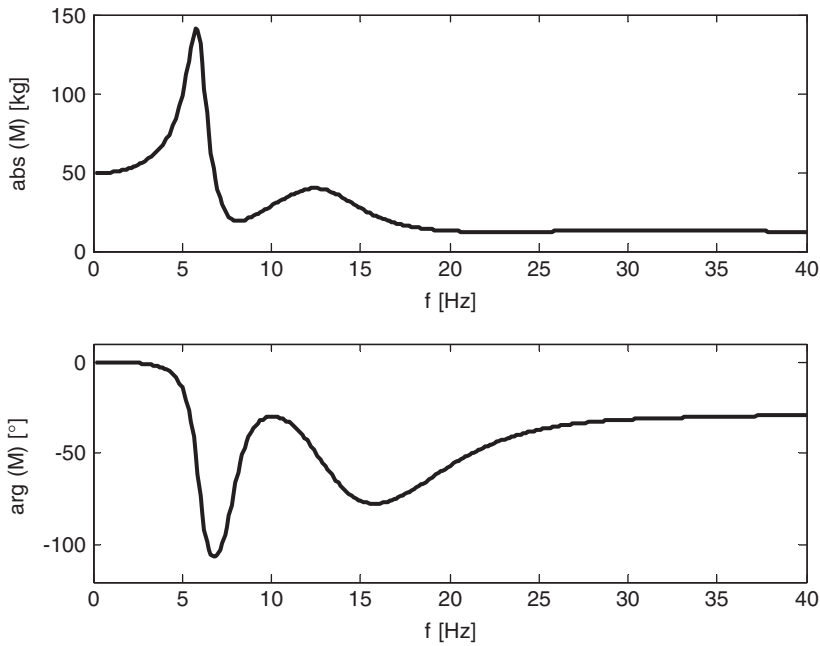


Fig. 7. Apparent mass of both 3 dof models (Fig. 6).

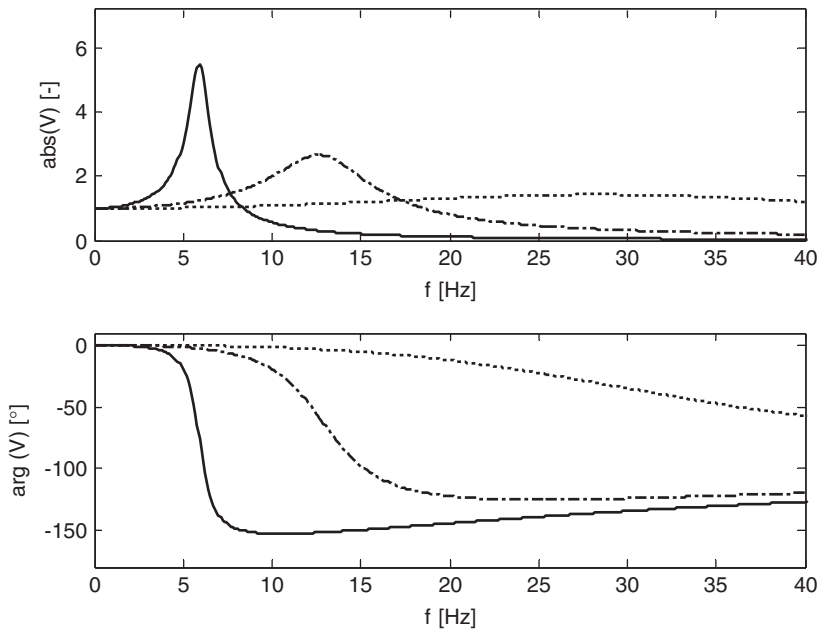


Fig. 8. Frequency response functions of the modal 3 dof model. — V_1 , - - - V_2 , V_3 .

The natural frequencies ω_r are the absolute values of the eigenvalues and damping ratios D_r are the ratio of the real part of the eigenvalue to the respective natural frequency. The natural frequencies and damping ratios can be found in Table 1. These parameters are used in the frequency response functions $V_r(\Omega)$ which contribute to the apparent mass. Fig. 8 illustrates the response function of each sdof system.

The generalized masses are computed using the modal matrix $\tilde{\Phi} = [\boldsymbol{\varphi}_1 \dots \boldsymbol{\varphi}_r \dots \boldsymbol{\varphi}_n]$ which contains all eigenvectors

$$\mathbf{M}^{\text{gen}} = \Phi^T \mathbf{M} \Phi. \quad (14)$$

Since the values of the eigenvectors define a ratio only, the modal matrix is usually scaled, e.g., the largest displacement, or rotation entry in each vector is unity. A normalization which is based on mass participation factors is applied to the modal matrix. Each eigenvector is normalized using each component of the diagonal generalized mass matrix:

$$\tilde{\boldsymbol{\varphi}}_r = \boldsymbol{\varphi}_r \frac{1}{m_r^{\text{gen}}} \boldsymbol{\varphi}_r^T \mathbf{M} \text{diag}(\mathbf{I}). \quad (15)$$

It is obvious that the sum of each row of the normalized modal matrix equals 1:

$$\tilde{\Phi} = \begin{bmatrix} 1.2989 & -0.3048 & 0.0059 \\ 0.3559 & 0.7743 & -0.1302 \\ 0.1283 & 0.3234 & 0.5483 \end{bmatrix}. \quad (16)$$

With the modified modal matrix $\tilde{\Phi}$, the modal masses (in (kg)), sometimes called modal effective masses, can then be calculated by analogy to Eq. (9):

$$\mathbf{M}^m = \tilde{\Phi}^T \mathbf{M} \tilde{\Phi}. \quad (17)$$

The modal stiffness and the modal damping coefficients can now be computed as

$$k_r^m = \omega_r^2 m_r^m, \quad (18)$$

$$c_r^m = 2m_r^m \omega_r D_r. \quad (19)$$

All parameters of the modal model are listed in Table 1. The advantage of the normalization technique based on the mass participation factors is that the modal quantities can be used in physical coordinates, and not only in the modal domain. It may be taken into account that the base mass of the modal model is identical to the in series model as the same excitation q_s at the driving point is applied to both models.

With regard to the seat-to-head transmissibility, the uppermost mass m_1 of the series model can be regarded as the head, even if the dampers and springs do not correspond to physiological structures within the body. All transfer functions from the base to the masses m_1^m , m_2^m and m_3^m are plotted in Fig. 9.

The modal model makes the representation of a head a little more complicated. It is not possible to assign the motion of the head to one particular sdof structure. But the modal model includes the seat-to-head transfer function as well: Again, it is just based on the frequency response function of each system and the modal matrix. The components of the participation factor scaled matrix correspond to the modal masses. The seat-to-head transmissibility can be expressed as

$$\begin{bmatrix} H_{10}(\Omega) \\ H_{20}(\Omega) \\ H_{30}(\Omega) \end{bmatrix} = \tilde{\Phi} \begin{bmatrix} V_1(\Omega) \\ V_2(\Omega) \\ V_3(\Omega) \end{bmatrix} \quad (20)$$

or can be written as an analogy to the apparent mass in Eq. (3)

$$H_{q0}(\Omega) = \sum_{r=1} \tilde{\Phi}_{qr} V_r(\Omega). \quad (21)$$

The above equations reveal that the modal matrix is required to express the seat-to-head transfer function in terms of modal parameters. The method can be used if the eigenmodes are available from a finite element analysis. Kitazaki and Griffin [18] determined the mode shapes from an experimental modal analysis on eight individuals using a method proposed by Dobson [19].

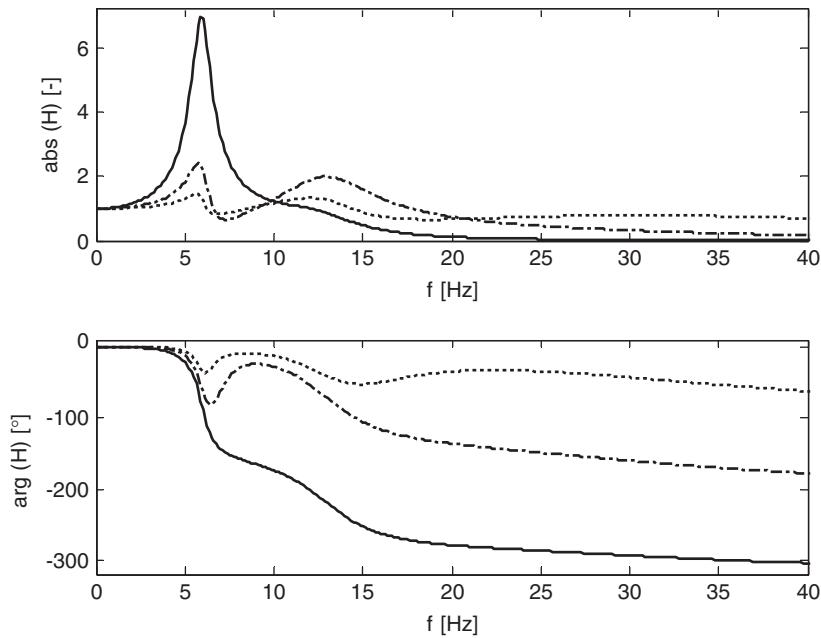


Fig. 9. Transfer functions of both 3 dof models (Fig. 6). — H_{10} , - - - H_{20} , H_{30} .

3. Results of the modally identified biodynamic response functions

To illustrate the abilities of the modal approach with respect to human vibration characteristics, the results of the six individual TP of the 50th male percentile (m 50) are presented. The experimental apparent mass data of Hinz et al. [20] was used.

Twenty-three males (body mass ranging from 58.2 to 106 kg, body height from 160.0 to 186.9 cm) and 22 females (51.5–84.1 kg, 154.0–175.0 cm) volunteered for the experiments. During vibration exposure, subjects were sitting on an anatomically shaped hard wooden seat coated with a thin layer of felt. The angle of the seat surface to the horizontal was 16° , the backrest of a commercial car seat was mounted independently of the seat surface at an angle of about 90° to the latter. The subjects sat in a relaxed and subjectively comfortable posture with both hands placed on the thighs near the knee joints and leaning against the backrest. Their feet rested on a support inclined 45° to the horizontal. The distance between this support and the seat was individually adjusted.

Three exposure conditions of random vertical whole-body vibration (frequency range 1–35 Hz, duration 130 s) were tested: E1—a nearly flat spectrum with 0.3 m s^{-2} rms (ISO 2631-1, 1997 [1]), E2 and E3—exposures with a spectrum measured under field conditions in a car with 0.7 and 1.4 m s^{-2} rms, respectively.

Table 2
Whole-body vibration characteristics with respect to listed parameters

Parameter	Symbol/name	Specification
Gender	M	Male
Mass percentile	50	Body mass: 72.7–77.5 kg mean body mass: 74.6 kg
Posture	Automotive	Position in a car
Direction of excitation	Z	Vertical
Intensity of excitation	E1	Broad-band excitation signal with 0.3 m s^{-2} rms
	E2	Spectrum measured under field conditions in a car with 0.7 m s^{-2} rms
	E3	Spectrum measured under field conditions in a car with 1.4 m s^{-2} rms

Data of the 50th male percentile and interacting parameters are summarized in Table 2.

It is not surprising that individual parameters can have a significant influence on the course of the apparent mass. Fig. 10 shows the modulus and the phase for six individuals (light dashed) for all three excitation intensities.

Table 3 shows the modally identified parameters of six TP at the same excitation signal (E2). It is obvious that the first peak occurs between 5.7 and 6.4 Hz. The second resonance frequency is located in the range of

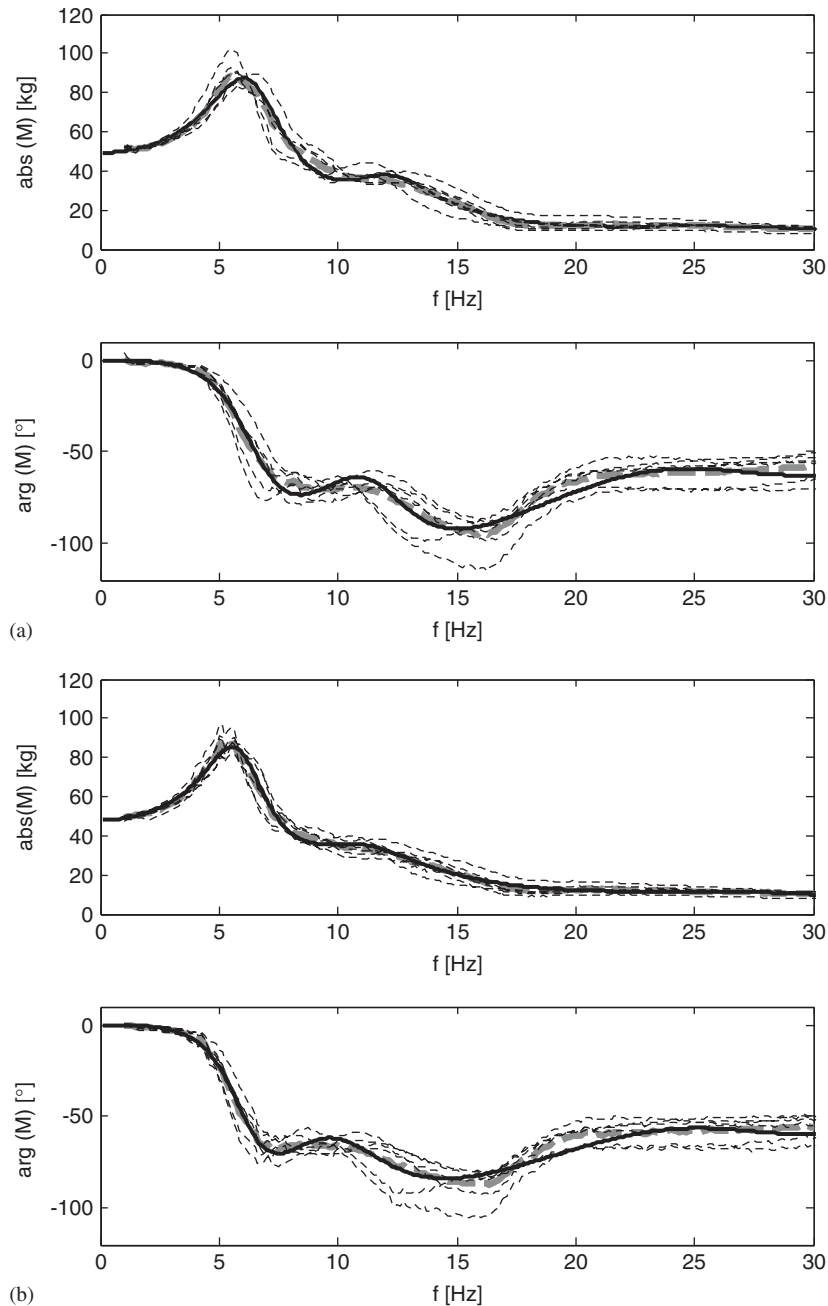


Fig. 10. Apparent mass of m 50 individuals, automotive posture, three excitation intensities: (a) E1, (b) E2 and (c) E3. — modally identified apparent mass, - - - mean apparent mass, - - - - individuals.

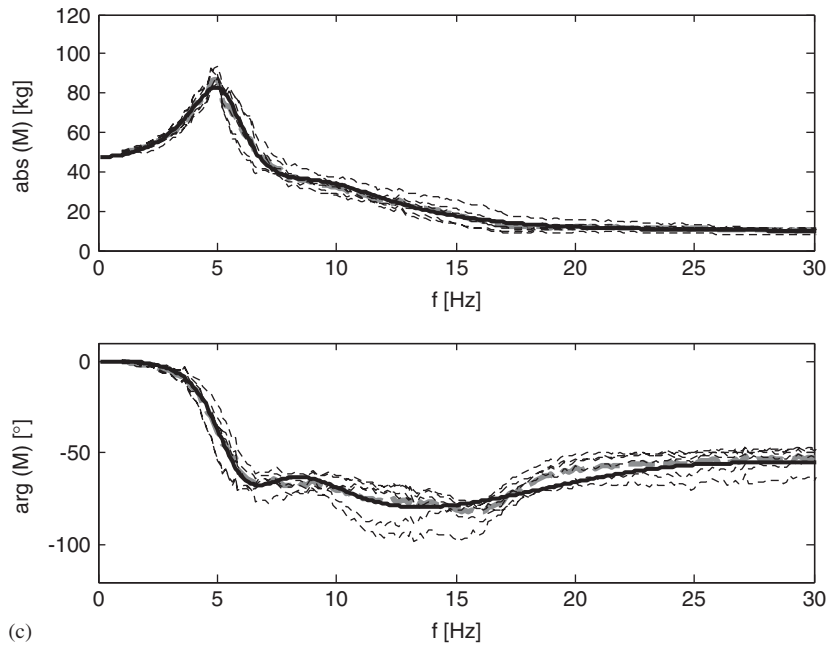


Fig. 10. (Continued)

Table 3
Modal parameters of m 50 individuals, automotive posture, excitation intensity E2

TP #	f_1 (Hz)	f_2 (Hz)	f_3 (Hz)	D_1 (%)	D_2 (%)	D_3 (%)	m_1^m (kg)	m_2^m (kg)	m_3^m (kg)	m_0^m (kg)
05	6.3	11.9	29.3	23	26	24	29.6	7.9	1.6	7.3
06	6.4	11.4	25.7	21	36	17	23.7	17.1	0.9	7.0
08	5.7	10.5	27.8	24	23	22	29.6	9.2	1.9	6.7
13	5.7	10.5	26.3	21	22	17	29.9	11.7	0.9	5.7
14	6.1	11.9	29.4	27	24	17	32.1	8.2	1.1	7.5
15	6.1	11.8	27.7	29	29	22	30.6	9.0	0.9	8.0
Mean \bar{x}	6.0	11.3	27.7	24	27	20	29.2	10.5	1.2	7.0
Std. dev. σ	0.30	0.66	1.52	3	5	3	2.89	3.50	0.41	0.78
COV \bar{x}/σ	4.9%	5.8%	5.5%	13.7%	19.6%	15.8%	9.9%	33.2%	34.0%	11.1%

12–13 Hz. Two TP (08 and 13) show some differences compared to the remaining subjects. Both peaks are shifted towards lower frequencies.

It is obvious that the identified natural frequencies only vary within a range of approximately 5% (coefficient of variation between 4.9% and 5.8%). The base mass and the first modal mass (contributing for the most part to the first peak) are usually concordant with all identified data sets, showing differences of roughly 10%. Significant differences between individuals are apparent in the second mass. The deviations of the damping ratios are relatively small because the anthropometrics of the TP did not differ significantly. However, the parameters describing the damping are ‘weaker’ than the resonant frequencies.

The mean apparent mass function, based on the modal identification of the individual curves, is compared to the ‘simple’ mean apparent mass (heavy dashed) in Fig. 10. While the first resonance frequency agrees very well in both averaging methods, the second main peak at 11.5 Hz shows some discrepancy.

The same procedure was extended to all three excitation signals while both the mass percentile and the posture were kept constant. Results of the modally identified and of the averaged apparent mass data sets are shown in Fig. 11. The upper and the lower boundaries of 18 separate apparent mass curves (six for each excitation intensity) are shown, since they underline the broad variety of individual data. Again, the second

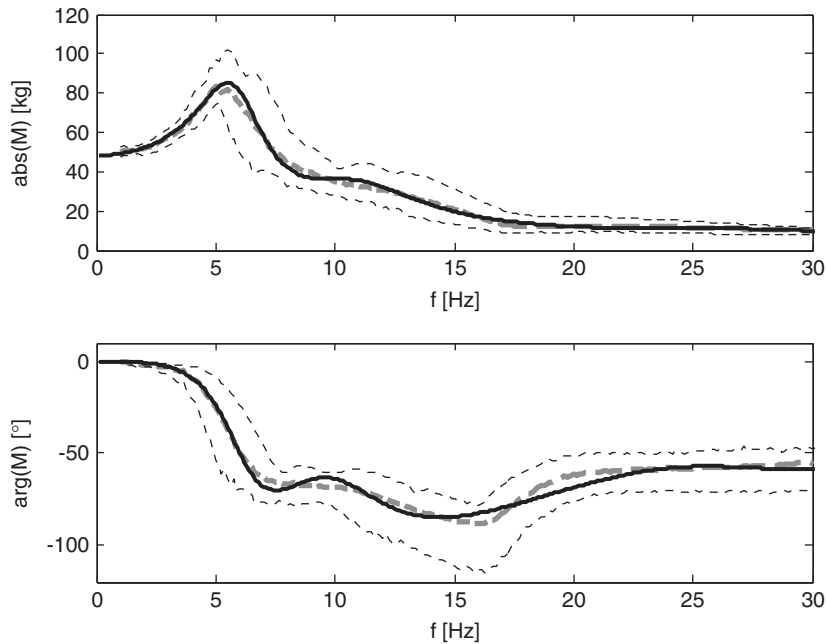


Fig. 11. Apparent mass of m_{50} individuals, automotive posture, averaged over all excitation intensities. — modally identified apparent mass, - - - mean apparent mass, ····· upper and lower bound.

peak of the averaged data is ‘smeared out’, while the modally identified curve preserves the information about the second main resonance.

4. Conclusions

The biodynamic response functions reported in the literature and the standards for the human body differ considerably. Much effort has been spent in analyzing, averaging, and smoothing measured data. Numerous mathematical models with different numbers of degrees of freedom and varying structures (configuration of multiple mass–spring–damper systems in series, in parallel or mixed) have been proposed. Parameters of these models were identified by fitting the model response to the measured input data. The quality of agreement between several models and target function was investigated to find the ‘best structure’, i.e. the structure which delivered the best fit. In some cases, special models were developed to deal with more than one response function, e.g. the apparent mass and the seat-to-head transmissibility function.

In this paper, the modal approach was introduced, in which the model consists of a base mass and n sdof structures. Comparison with a 3 dof in series model reveals that the modal model not only represents the “to-the-body” but also the “through-the-body” response characteristics, such as the seat-to-head response function.

Applying the method to real experimental data demonstrated that modal parameters such as natural frequencies, modal masses, and damping ratios can be identified from individual data sets. The modal description is an appropriate means to characterize the responses to whole body vibrations and to study the influence of different vibration conditions.

The problem of averaging different curves to achieve a mean function was addressed. The identified modal parameters should be used as a basis for calculating mean response functions because the main vibration characteristics will be preserved. It is not limited to the traditional method of comparing the height and the frequency range of the peaks. The set of modal parameters contains all the relevant information to describing the human vibration behavior and it can be used for statistical testing procedures.

Since the modal approach generates structures of the human body which are not restricted by an anatomical context, it is applicable for the development of phenomenological models. The mathematical model can be realized as a hardware design, the so-called hardware vibration dummy.

It has been general practice to compare computed response functions of simulation models, including finite element models, with experimental data by plotting the relevant curves. Further research is required to establish a ‘validation platform’ in terms of the basic dynamic properties, namely the modal parameters. Complex software models of the human body can be broken down to straightforward mathematical models using modal analysis tools. This method can be employed to render simulation and experimental data comparable, as well as to support the validation process for software models.

Acknowledgements

This study was supported by the German Federal Institute for Occupational Safety and Health in research project F2028 (joint research project with FIOSH).

References

- [1] International Organization for Standardization, Mechanical vibration and shock—Evaluation of human exposure to whole-body vibration—part 1: general requirements, *International Standard ISO 2631-1*, 1997.
- [2] Directive 2002/44/EC of the European Parliament and of the Council of 25 June 2002 on the minimum health and safety requirements regarding the exposure of workers to the risks arising from physical agents (vibration) (sixteenth individual Directive within the meaning of Article 16(1) of Directive 89/391/EEC).
- [3] R.R. Coermann, The mechanical impedance of the human body in sitting and standing position at low frequencies, *Human Factors* 4 (1962) 227–253.
- [4] C.W. Suggs, L.F. Strikeleather, J.Y. Harrison, R.E. Young, Application of a Dynamic Simulator in Seat Testing, *Am Soc Agric Eng* (1969) 69–172.
- [5] T.E. Fairly, M.J. Griffin, The apparent mass of the seated human body: vertical vibration, *Journal of Sound and Vibration* 22 (1989) 81–94.
- [6] J. Knoblauch, Entwicklung und Bau eines physikalischen Schwingungsmodells des sitzenden Menschen, *Shaker Verlag*, 1992.
- [7] P.-É. Boileau, S. Rakheja, X. Wu, A body mass dependent mechanical impedance model for applications in vibration seat testing, *Journal of Sound and Vibration* 253 (2002) 243–264.
- [8] L. Wei, M.J. Griffin, Mathematical models for the apparent mass of the seated human body exposed to vertical vibration, *Journal of Sound and Vibration* 212 (1998) 855–874.
- [9] International Organization for Standardization, Mechanical vibration and shock—range of idealized values to characterize seated-body biodynamic response under vertical vibration, *International Standard ISO 5982*, 2001.
- [10] N.J. Mansfield, R. Lundström, Models of the apparent mass of the seated human body exposed to horizontal whole-body vibration, *Aviation, Space, and Environmental Medicine* 70 (1999) 1166–1172.
- [11] B. Hinz, R. Blüthner, G. Menzel, S. Rützel, H. Seidel, H.P. Wölfel, Apparent mass of seated men—determination with single-axis and multi-axes excitations at different magnitudes, *Journal of Sound and Vibration*, 2005, this issue.
- [12] The Mathworks Inc., *MATLAB*, Release 14, 2004.
- [13] X. Wu, S. Rakheja, P.-É. Boileau, Analyses of relationships between biodynamic response functions, *Journal of Sound and Vibration* 226 (1999) 595–606.
- [14] Deutsche Industrienorm, Mechanical impedances at the driving point and transfer functions of the human body, *German Standard DIN 45676*, 2003.
- [15] T.K. Hasselman, Method for constructing a full modal damping matrix from experimental measurements, *AIAA Journal* 10 (1972) 526–527.
- [16] D.F. Pilkey, D.J. Inman, An iterative approach to viscous damping matrix identification, *Proceedings of the 15th International Modal Analysis Conference*, 1997, 1152–1157.
- [17] S. Naylor, J.E. Cooper, J.R. Wright, On the estimation of modal matrices with non-proportional damping, *Proceedings of the 15th International Modal Analysis Conference*, 1997, 1371–1378.
- [18] S. Kitazaki, M.J. Griffin, Resonance behaviour of the seated human body and effects of posture, *Journal of Biomechanics* 31 (1998) 143–149.
- [19] B.J. Dobson, A straight-line technique for extracting modal properties from frequency response data, *Mechanical Systems and Signal Processing* 1 (1987) 29–40.
- [20] B. Hinz, H. Seidel, G. Menzel, L. Gericke, R. Blüthner, J. Keitel, Seated occupant apparent mass in automotive posture—examination with groups of subjects characterised by a representative distribution of body mass and body height, *Zeitschrift für Arbeitswissenschaft* 4 (2004) 249–264 (in German).